Identification of fractional-order transfer functions and nonzero initial conditions using exponentially modulated signals

OPEN ACCESS
IOP Publishing
Measurement Science and Technology
Meas. Sci. Technol. **36** (2025) 016036 (8pp)
https://doi.org/10.1088/1361-6501/ad903d

Identification of fractional-order transfer functions and nonzero initial conditions using exponentially modulated signals

Hadamez Kuzminskas[1], Marcelo Carvalho Minhoto Teixeira[1], Roberto Kawakami Harrop Galvão[2], Edvaldo Assunção[1] and Sillas Hadjiloucas[3,*]

[1] Department of Electrical Engineering, São Paulo State University (UNESP), Ilha Solteira, SP, 15385-007, Brazil
[2] Electronics Engineering Division, Instituto Tecnológico de Aeronáutica (ITA), São José dos Campos 12228-900, SP, Brazil
[3] School of Biological Sciences, Department of Biomedical Engineering, The University of Reading, Reading RG6 6AY, United Kingdom

E-mail: s.hadjiloucas@reading.ac.uk

Received 13 January 2024, revised 4 October 2024
Accepted for publication 8 November 2024
Published 29 November 2024

Abstract

A new methodology that uses exponentially modulated signals with arbitrary excitation waveforms for the identification of fractional order transfer functions is proposed. In contrast to previous approaches where initial conditions were not considered and the system was required to be at rest for the identification procedure, the current contribution extends the formulation to the case where the system has non-zero initial conditions, dispensing with the need to place it at a resting state. This generalization is important in feedback instrumentation and metrology applications where the measurement or control process may not be disrupted to perform identification. Moreover, the procedure has a broader scope of applications because it structurally contemplates the case when the model presents derivatives in the input. Full identification of the system parameters as well as the fractional exponents associated with the model dynamics are achieved through a grid search procedure with resolution adjustable by the user. Two simulation examples are presented to illustrate the effectiveness of the proposed approach. The first example is concerned with the effect of measurement noise at the observed system output, whereas the second involves the identification of the impedance of a three-dimensional RC network model. These types of RC networks have dynamics capturing complex phenomena with emergent responses and are ideal for emulating the complex dynamics encountered across physical sciences and in particular interdisciplinary subject areas such as biomedical engineering.

Keywords: fractional order systems, system identification, transfer functions, nonzero initial conditions, system dynamics

* Author to whom any correspondence should be addressed.

1. Introduction

Fractional order systems have drawn much interest in the literature and are in the process of becoming more embedded in real-world applications because of their ability to capture complex phenomena from a system dynamics perspective [1–3]. In this context, the present work is concerned with the identification of fractional-order models through the use of exponentially modulated input/output signals [4, 5]. This concept was originally introduced in [4] for the identification of the parameters and fractional exponents of a transfer function from step response measurements. A generalization that allowed for the use of arbitrary input waveforms was later presented in [5]. Both papers assumed that the system was initially at rest, which may not be possible in actual identification experiments. The current contribution extends the results of [5] to the case where the system has nonzero initial conditions, which was also addressed in [6], through the use of block pulse functions. However, the approach proposed herein has a broader scope of application compared with [6], because it can handle models with derivatives at the input and also allows for the identification of the fractional exponents. In [7], the block pulse method developed in [6] was extended to deal with derivatives at the input, as well as unknown time delays, but no example actually involving the input derivatives was presented. In addition, the fractional exponents were assumed to be known, as in [6]. The issue of nonzero initial conditions was also considered in a more recent paper [8] for models in pseudo-state space form. However, that study was restricted to models of commensurate order, whereas the present contribution allows for the use of non-conmmensurate exponents in the transfer function to be identified.

The remainder of this contribution is organized as follows. Section 2 introduces some mathematical concepts and presents a theorem that serves as the basis for the identification method proposed in section 3. A numerical example is shown in section 4 and conclusions are given in section 5. Throughout the text, the set of positive integers will be represented by $\mathbb{N}^+ = \{1,2,\ldots\}$. Given $\alpha \in \mathbb{R}$, the smallest integer greater than or equal to α will be denoted by $\lceil \alpha \rceil$.

2. Preliminary concepts

Different types of fractional-order derivatives are found in the literature, including the Caputo, Riemann–Liouville (which is equivalent to the Grünwald–Letnikov derivative under certain conditions) [9], and Hadamard [10, 11] definitions. Within the scope of the present work, the Caputo derivative is more convenient because the initial conditions can be expressed in terms of integer-order derivatives [12] and the usual properties of the Laplace transform apply. In contrast, the initial conditions with the Riemann–Liouville derivative are expressed in terms of fractional-order derivatives and the Hadamard derivative requires the use of a modified Laplace transform because the differentiation begins at an initial instant different from zero [13].

Consider the following fractional differential equation using the Caputo derivative [9]:

$$\sum\nolimits_{i=1}^{n} a_i {}^{c}D^{\alpha_i} y(t) + y(t) = \sum\nolimits_{j=1}^{m} b_j {}^{c}D^{\beta_j} u(t) + b_0 u(t) \quad (1)$$

with a given number of real-valued coefficients $a_1, \ldots, a_n$, b_0, $b_1, \ldots, b_m$, and real-valued exponents $0 < \alpha_1 < \cdots < \alpha_n$, $0 < \beta_1 < \cdots < \beta_m$, with $\beta_m < \alpha_n$.

Let $U(s) = \mathcal{L}\{u(t)\}$ and $Y(s) = \mathcal{L}\{y(t)\}$ denote the Laplace transforms of the input and output signals, respectively. The Laplace transform of ${}^{c}D^{\alpha} y(t)$ is $\mathcal{L}\{{}^{c}D^{\alpha} y(t)\} = s^{\alpha} Y(s) - \sum_{k=0}^{p_\alpha - 1} s^{\alpha-k-1} y^{(k)}(0^-)$, with $p_\alpha - 1 < \alpha < p_\alpha$ and $p_\alpha \in \mathbb{N}^+$ [9]. By applying this transform in (1), with initial conditions $y^{(k)}(0^-)$, $k = 0, 1, \ldots, p_{\alpha_n} - 1$ and $u^{(l)}(0^-) = 0$, $l = 0, 1, \ldots, p_{\beta_m} - 1$, it follows that

$$Y(s) = G(s)\, U(s) + H(s) \quad (2)$$

with

$$G(s) = \frac{b_0 + b_1 s^{\beta_1} + \cdots + b_m s^{\beta_m}}{1 + a_1 s^{\alpha_1} + \cdots + a_n s^{\alpha_n}}, \quad (3)$$

$$H(s) = \frac{\sum_{i=1}^{n} a_i \sum_{k=0}^{p_{\alpha_i}-1} s^{\alpha_i - k - 1} y^{(k)}(0^-)}{1 + a_1 s^{\alpha_1} + \cdots + a_n s^{\alpha_n}} = \frac{\sum_{i=1}^{n} \sum_{k=0}^{p_{\alpha_i}-1} s^{\alpha_i - k - 1} f_{i_k}}{1 + a_1 s^{\alpha_1} + \cdots + a_n s^{\alpha_n}} \quad (4)$$

where

$$f_{i_k} = a_i y^{(k)}\left(0^-\right); i = 1, 2, \ldots, n; k = 0, 1, \ldots, p_{\alpha_i} - 1. \quad (5)$$

The basic idea of the proposed identification method consists of rewriting (2) in the form $Y(s) = \bar{G}(s) U(s)$, with

$$\bar{G}(s) = G(s) + U(s)^{-1} H(s). \quad (6)$$

Therefore, the problem can be recast as the identification of an equivalent artificial system with transfer function $\bar{G}(s)$ and null initial conditions. The proposed identification method uses the auxiliary signals $z(t)$ and $w(t)$ (dependent on a positive parameter $\sigma \in \mathbb{R}$), which are obtained by the exponential modulation procedure depicted in figure 1, similarly to the approach presented in [5].

The following theorem provides the relationship among the values $\lim_{t\to\infty} z(t) = z_\infty$, $\lim_{t\to\infty} w(t) = w_\infty$ and the parameters in (3) and (4).

Theorem 1. *If $\sigma > 0$ is such that z_∞ and w_∞ exist, then*

$$z_\infty = w_\infty G(\sigma) + \sigma H(\sigma). \quad (7)$$

Proof 1. From figure 1, $Z(s) = [(s+\sigma)/s]\mathcal{L}\{y(t)\mathrm{e}^{-\sigma t}\} = [(s+\sigma)/s] Y(s+\sigma)$. Since $Y(s) = \bar{G}(s) U(s)$, it follows that $Z(s) = [(s+\sigma)/s]\bar{G}(s+\sigma) U(s+\sigma)$. From the Final Value Theorem, $z_\infty = \lim_{s\to 0} sZ(s)$, and thus $z_\infty = \sigma \bar{G}(\sigma) U(\sigma)$.

Similarly, $W(s) = (\sigma/s)\mathcal{L}\{u(t)\mathrm{e}^{-\sigma t}\} = (\sigma/s)U(s+\sigma)$, and thus $w_\infty = \lim_{s\to 0} sW(s) = \sigma U(\sigma)$. In view of these expressions for z_∞ and w_∞, note that $z_\infty = w_\infty \bar{G}(\sigma)$. Now, considering (6) and using $U(\sigma)^{-1} = \sigma/w_\infty$, one arrives in (7). □

Remark 1. The assumption $\beta_m < \alpha_n$ adopted herein implies that the transfer function (3) is strictly proper and thus the frequency-domain gain $|G(j\omega)|$ vanishes as $\omega \to \infty$.

3. Proposed identification method

From (3), (4) and theorem 1, it follows that

$$z_\infty\left(a_1\sigma^{\alpha_1} + \cdots + a_n\sigma^{\alpha_n}\right) - w_\infty\left(b_0 + b_1\sigma^{\beta_1} + \cdots + b_m\sigma^{\beta_m}\right) - \sum_{i=1}^{n}\sum_{k=0}^{p_{\alpha_i}-1} f_{i_k}\sigma^{\alpha_i-k} = -z_\infty. \tag{8}$$

By adopting $q = 2(n+m+1+\sum_{i=1}^{n} p_{\alpha_i})$ different values of the parameter $\sigma = \sigma_i$ in figure 1, one obtains z_{i_∞}, w_{i_∞}, $i = 1,2,\cdots,q$, as in [5]. Therefore, the identification problem can be addressed on the basis of the following equation:

$$A\theta = c + e \tag{9}$$

$$A = \begin{pmatrix} z_{1_\infty}\sigma_1^{\alpha_1} & \cdots & z_{1_\infty}\sigma_1^{\alpha_n} & -w_{1_\infty} & -w_{1_\infty}\sigma_1^{\beta_1} & \cdots & -w_{1_\infty}\sigma_1^{\beta_m} \\ z_{2_\infty}\sigma_2^{\alpha_1} & \cdots & z_{2_\infty}\sigma_2^{\alpha_n} & -w_{2_\infty} & -w_{2_\infty}\sigma_2^{\beta_1} & \cdots & -w_{2_\infty}\sigma_2^{\beta_m} \\ \vdots & \vdots & \vdots & \vdots & \vdots & \vdots & \vdots \\ z_{q_\infty}\sigma_q^{\alpha_1} & \cdots & z_{q_\infty}\sigma_q^{\alpha_n} & -w_{q_\infty} & -w_{q_\infty}\sigma_q^{\beta_1} & \cdots & -w_{q_\infty}\sigma_q^{\beta_m} \end{pmatrix}$$
$$\begin{pmatrix} -\sigma_1^{\alpha_1} & \cdots & -\sigma_1^{\alpha_1-p_{\alpha_1}+1} & \cdots & -\sigma_1^{\alpha_n} & \cdots & -\sigma_1^{\alpha_n-p_{\alpha_n}+1} \\ -\sigma_2^{\alpha_1} & \cdots & -\sigma_2^{\alpha_1-p_{\alpha_1}+1} & \cdots & -\sigma_2^{\alpha_n} & \cdots & -\sigma_2^{\alpha_n-p_{\alpha_n}+1} \\ \vdots & \vdots & \vdots & \vdots & \vdots & \vdots & \vdots \\ -\sigma_q^{\alpha_1} & \cdots & -\sigma_q^{\alpha_1-p_{\alpha_1}+1} & \cdots & -\sigma_q^{\alpha_n} & \cdots & -\sigma_q^{\alpha_n-p_{\alpha_n}+1} \end{pmatrix} \tag{10}$$

$$\theta = \begin{bmatrix} a_1 & \cdots & a_n & b_0 & \cdots & b_m & f_{1_0} & \cdots & f_{1_{p_{\alpha_1}-1}} & \cdots & f_{n_0} & \cdots & f_{n_{p_{\alpha_n}-1}} \end{bmatrix}^{\mathrm{T}} \tag{11}$$

$$c = -\begin{bmatrix} z_1(\infty) & z_2(\infty) & \cdots & z_q(\infty) \end{bmatrix}^{\mathrm{T}} \tag{12}$$

where $A \in \mathbb{R}^{q\times q/2}$ is the matrix of regressors and e is the model error associated to the presence of noise in the measurements. A least-squares estimate of the parameter vector θ is then obtained as

$$\hat{\theta} = \left(A^{\mathrm{T}}A\right)^{-1}A^{\mathrm{T}}c. \tag{13}$$

Now, let $\hat{e} = A\hat{\theta} - c$ be the vector of identification residuals. In order to determine suitable values for the fractional exponents $\alpha_1,\ldots,\alpha_n$, $\beta_1,\ldots,\beta_m$, we shall consider the sum square error $E = \hat{e}^{\mathrm{T}}\hat{e}$ derived from (13) as

$$\begin{aligned} E &= \left(A\hat{\theta} - c\right)^{\mathrm{T}}\left(A\hat{\theta} - c\right) \\ &= c^{\mathrm{T}}\left[A\left(A^{\mathrm{T}}A\right)^{-1}A^{\mathrm{T}}A\left(A^{\mathrm{T}}A\right)^{-1}A^{\mathrm{T}} - 2A\left(A^{\mathrm{T}}A\right)^{-1}A^{\mathrm{T}} + I\right]c \\ &= c^{\mathrm{T}}\left[I - A\left(A^{\mathrm{T}}A\right)^{-1}A^{\mathrm{T}}\right]c. \end{aligned} \tag{14}$$

A gridding procedure similar to [5] can then be employed as described below. To this end, it is assumed that $\beta_m < \alpha_n$, as stated in section 2, and that an upper bound $\alpha_{\max} \in \mathbb{N}^+$ on the values of α_i is known.

Step 1) Find the minimum value of E over a grid of values for the fractional exponents, with $0 < \alpha_1 < \cdots < \alpha_n$, $0 < \beta_1 < \cdots < \beta_m < \alpha_n$, and $\alpha_i < \alpha_{\max}$, $i = 1,2,\ldots,n$. At each grid point, the number of parameters f_{i_k} is given by $p_{\alpha_i} = \lceil \alpha_i \rceil$ for each $i = 1,2,\ldots,n$.

Step 2) Let $\hat{\theta} = \begin{bmatrix}\hat{a}_1 \cdots \hat{a}_n\ \hat{b}_0 \cdots \hat{b}_m \hat{f}_{1_0} \cdots \hat{f}_{n_{p_{\alpha_n}-1}}\end{bmatrix}^{\mathrm{T}}$ be the vector of parameter estimates obtained as the result of **Step 1**. Now let $\mathbb{S}_k$ be an index set defined as

$$\mathbb{S}_k = \{i \in \{1,2,\ldots,n\} \,:\, p_{\alpha_i} - 1 \geqslant k\} \tag{15}$$

for each $k = 0,1,\ldots,p_{\alpha_i-1}$. In view of (5), one can write regression equations for the estimation of $y^{(k)}(0^-)$ in the form

$$\hat{f}_{i_k} = \hat{a}_i y^{(k)}\left(0^-\right) + \tilde{e}_{i_k},\ i \in \mathbb{S}_k \tag{16}$$

where $\tilde{e}_{i_k}$ is an error term. From (16), a least-squares estimate for $y^{(k)}(0^-)$ is then given by

$$\hat{y}^{(k)}\left(0^-\right) = \left(\sum_{i\in\mathbb{S}_k}\hat{a}_i^2\right)^{-1}\sum_{i\in\mathbb{S}_k}\hat{a}_i\hat{f}_{i_k} \tag{17}$$

for $k = 0,1,\ldots,p_{\alpha_n-1}$.

Remark 2. In practice, the identification outcome may be affected by the choice of σ_i values owing to the presence of measurement noise and the finite-length nature of the

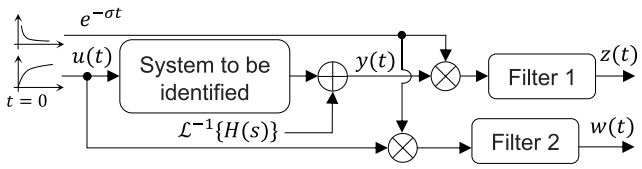

Figure 1. Generation of the signals used in the proposed method. The transfer functions of the blocks 'System to be identified', 'Filter 1' and 'Filter 2' are, respectively, $G(s)$, $(\sigma+s)/s$ and σ/s. The circles with $\times$ and $+$ signs indicate pointwise multiplication and addition in the time domain. $\mathcal{L}^{-1}\{H(s)\}$ represents the inverse Laplace transform of $H(s)$.

input/output data set. Indeed, small σ_i values will result in a slow convergence of the auxiliary signals $z_i(t)$ and $w_i(t)$, thus compromising the accurate determination of z_{i_∞} and w_{i_∞} within the time span of the data. In contrast, if the σ_i values are too large, the determination of z_{i_∞} and w_{i_∞} will depend almost exclusively on the early part of the input/output signals, as if the identification data spanned a shorter time interval. This is not convenient either, as the effect of measurement noise tends to be more pronounced if shorter data sets are employed.

Remark 3. Other types of modulating functions $f(t)$ could be employed in the proposed method as an alternative to $f(t) = \exp(-\sigma t)$, provided that $\int_0^t y(\tau)f(\tau)\mathrm{d}\tau$ and $\int_0^t u(\tau)f(\tau)\mathrm{d}\tau$ converge to limit values as $t \to \infty$ to warrant the use of the Final Value Theorem. Examples include functions of the form $f(t) = \exp(-(\sigma + j\omega)t)$ with different values of σ and ω. However, this possibility is left for future research.

Remark 4. As an alternative to a grid search procedure, suitable values of $\alpha_1, \ldots, \alpha_n, \beta_1, \ldots, \beta_m$ could be determined by using numerical optimization techniques such as the well-known Nelder–Mead (also known as polytope) algorithm [14], as discussed in [5].

4. Examples

4.1. Example 1

The proposed method was implemented in the MATLAB® software. Moreover, the FOTF computational package [15] was employed to generate identification data through numerical simulations of a fractional-order system. Let $G(s) = (b_0 + b_1 s^{\beta_1})/(1 + a_1 s^{\alpha_1})$ be the transfer function of the system to be identified, with $a_1 = 5$, $b_0 = 2$, $b_1 = 3, \alpha_1 = 1.5$, $\beta_1 = 0.9$, $y(0^-) = 1$ and $\dot{y}(0^-) = -1$. The system was excited by using an input signal $u(t) = \sum_{i=1}^{3} \sin(\pi t/(5(i+1)))$ over a time span of 200 s with a simulation time step of 0.005 s. The resulting output $y(t)$ was corrupted with Gaussian noise of zero mean and standard deviation of 0.1. The input and output signals thus obtained are presented in figures 3(a) and (b), respectively.

Figure 2 presents the auxiliary signals $z_1(t)$ and $w_1(t)$ for five different values of σ_1. The central value $\sigma_1 = \ln(100)/200$ corresponds to a 100-fold decay of the exponential $\mathrm{e}^{-\sigma_1 t}$ over the identification time span. In order to reduce the error in the

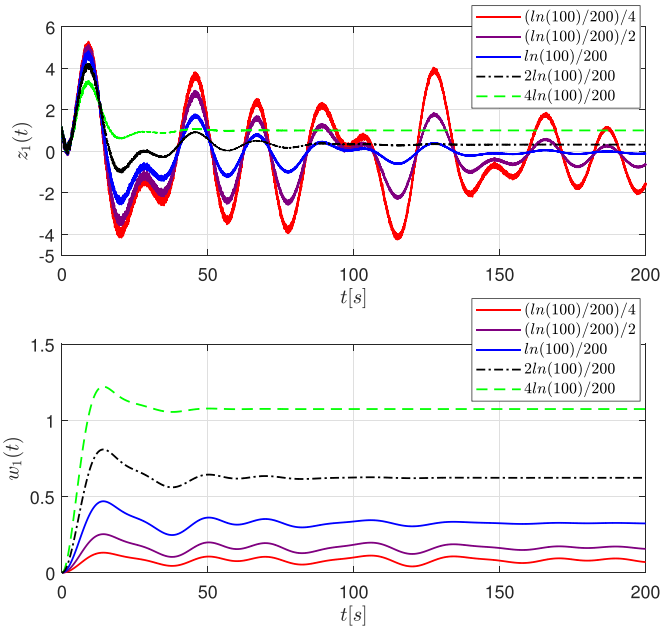

Figure 2. Auxiliary signals $z_1(t)$ and $w_1(t)$ for five different values of σ_1 (indicated in the legend).

determination of the limit values z_∞ and w_∞, we adopted $\sigma_1 = 2\ln(100)/200 = 0.0461$ (dash-dotted lines in figure 2), which was also the recommendation stated in [5]. Again in line with [5], the remaining σ_i values were calculated as $\sigma_i = \sigma_{i-1}^{1/2}$, $i = 2, 3, \ldots, q$, so that $\sigma_1 < \sigma_2 < \cdots < \sigma_q$, thus ensuring a suitable determination of z_{i_∞} and w_{i_∞}.

The grid search procedure in **Step 1** was implemented with $\alpha_{\max} = 2$ and a step of 0.1 in both α_1 and β_1. As shown in figure 3(c), the minimal value $E = 8.2 \times 10^{-10}$ was obtained for $\hat{\alpha}_1 = 1.5$ and $\hat{\beta}_1 = 0.9$, which correspond to the actual values of the fractional exponents. The identified transfer function was

$$\hat{G}(s) = \frac{\hat{b}_0 + \hat{b}_1 s^{\hat{\beta}_1}}{1 + \hat{a}_1 s^{\hat{\alpha}_1}} = \frac{1.9992 + 2.9959 s^{0.9}}{1 + 5.0043 s^{1.5}}. \qquad (18)$$

By following **Step 2** of the proposed procedure, the initial conditions were estimated as $\hat{y}(0^-) = 1.0061$ and $\hat{\dot{y}}(0^-) = -0.9977$.

The reproducibility of the results was investigated by repeating the identification 2000 times, each time with a different noise realization, under the same conditions of the simulation described above. As can be seen in table 1 and figure 4, the estimates obtained with the proposed method did not exhibit bias with respect to the actual values of the parameters and initial conditions. Moreover, the estimates displayed small dispersion, with relative standard deviations no larger than 6 %. For comparison, table 1 also presents the identification results obtained with the method described in [5], which assumes null initial conditions. Note that disregarding the initial conditions led to considerable errors in the parameter estimates.

The effect of increasing the amplitude of the measurement noise up to four times is illustrated in figures 5 and 6. As can be seen, the outcome consists of a general degradation of the

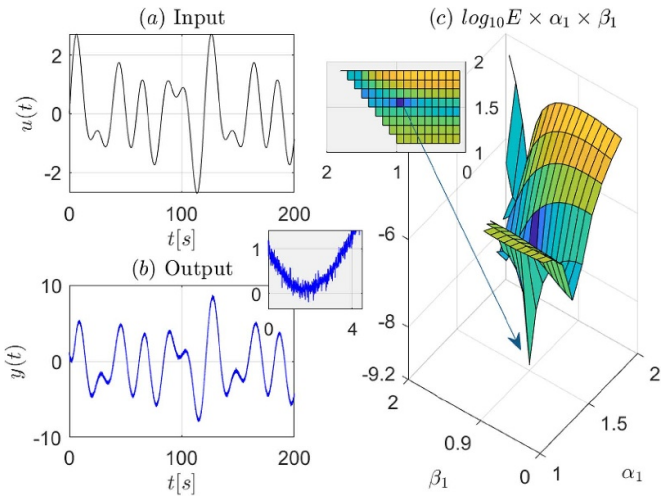

Figure 3. (a) Input signal, (b) output signal, (c) index E employed in the determination of α_1 and β_1. The inset presents a top view of the three dimensional plot, with the dark blue square corresponding to the minimum value of E.

Table 1. Identification results (mean ± standard deviation over 2000 runs) obtained with the proposed method and with the method presented in [5].

Parameter	Proposed method	Method in [5]	Actual value
α_1	1.5 ± 0	1.1 ± 0	1.5
β_1	0.90 ± 0.05	1.0 ± 0	0.9
a_1	4.99 ± 0.08	-3.9 ± 0.1	5
b_0	2.00 ± 0.06	0.860 ± 0.007	2
b_1	3.0 ± 0.1	-2.93 ± 0.05	3
$y(0^-)$	1.00 ± 0.01	–	1
$\dot{y}(0^-)$	-1.00 ± 0.04	–	-1

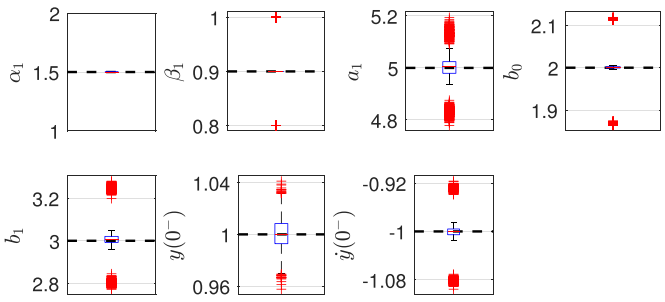

Figure 4. Variation in the identification results using the proposed method. The blue boxes comprise the 25th and 75th percentiles, with the central red line corresponding to the median and bars extending to extreme points. Outliers are indicated by cross markers.

estimates in terms of bias and dispersion. Interestingly, the estimates of β_1, b_0, b_1, which are associated with the numerator of $G(s)$, were more sensitive to noise compared with the estimates of α_1 and a_1, which are associated with the denominator of $G(s)$. By using concepts from classical control theory [16], one may argue that the dynamical features of the system are more strongly related to the denominator of $G(s)$. Therefore, it stands to reason that the parameter estimates

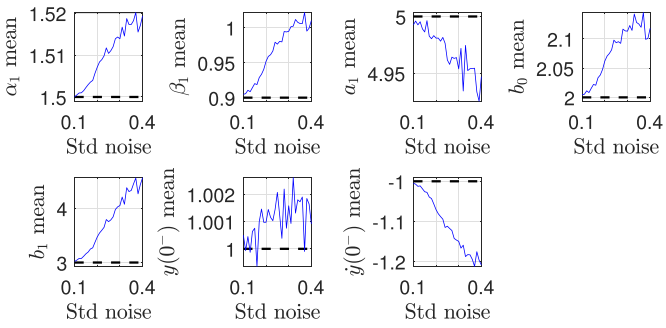

Figure 5. Mean of the α_1, β_1, a_1, b_0, b_1, $y(0^-)$, $\dot{y}(0^-)$ estimates as identified through the proposed method. Plots show how an increase in the standard deviation of noise in the output signal of the fractional order system affects the calculated value for each parameter. The actual value of the parameter is indicated by a dashed line in each plot.

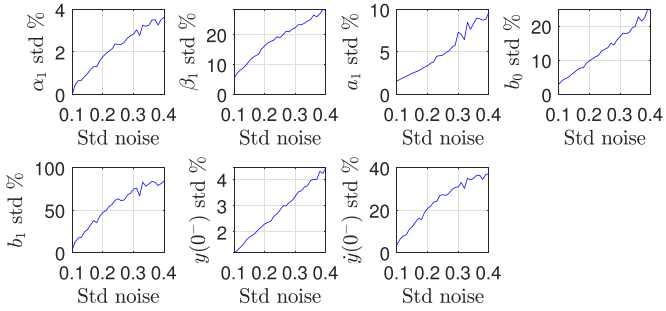

Figure 6. Relative standard deviation (standard deviation divided by mean, in percentage) of the α_1, β_1, a_1, b_0, b_1, $y(0^-)$, $\dot{y}(0^-)$ estimates for increasing values of the standard deviation of noise in the output signal $y(t)$.

associated with the denominator are less affected by the measurement noise. Figures 5 and 6 also reveal that the estimate of $y(0^-)$ was less sensitive to noise compared with the estimate of $\dot{y}(0^-)$. This finding can be interpreted by noting that $y(0^-)$ is directly measured, whereas $\dot{y}(0^-)$ is not. Research is under way to reduce the overall sensitivity of the proposed method with respect to noise.

4.2. Example 2: three-dimensional RC network

This second example involves the three-dimensional RC network model presented in [17], which was also used as a case study in [4]. The network was configured with five layers of 3×5 nodes between the external electrodes and an excitation source with internal resistance $R_S = 0.1\ \Omega$, as shown in figure 7. Each dashed line connecting a pair of nodes in the network represents either a resistor or a capacitor, with normalized component values $R = 1\ \Omega$, $C = 0.5$ F. The R and C components were randomly allocated throughout the network, with equal fractions of each component type.

The system-theoretic approach employed in [17] yielded a model of the form

$$\mathrm{d}z(t)/\mathrm{d}t = Fz(t) + Nu_S(t) \tag{19}$$

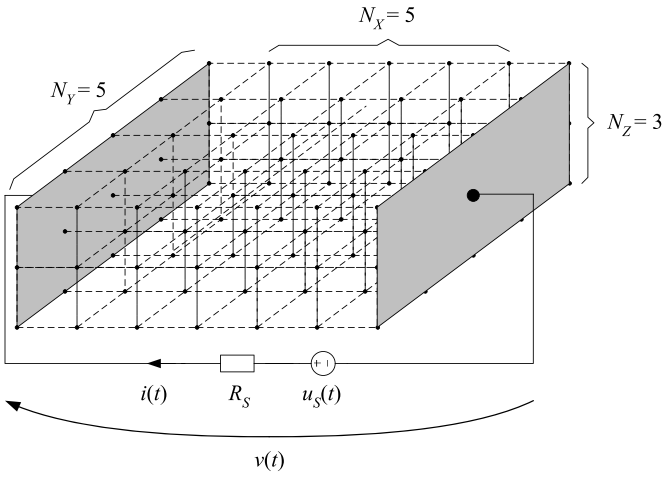

Figure 7. Three-dimensional network employed in example 2. Each dashed line connecting a pair of nodes can be either a resistor or a capacitor.

$$i(t) = Hz(t) + Lu_S(t) \tag{20}$$

where $z(t)$ is the state vector, the scalars $u_S(t)$, $i(t)$ are the source voltage and the current entering the network at time t, $L = 1/R_S$, and F, N, H are matrices of compatible dimensions. The complex network admittance (including the source resistance R_S) was then calculated as $Y(j\omega) = H(j\omega I - F)^{-1}N + L$ at each angular frequency ω. As shown in [17], the magnitude $|Y(j\omega)|$ increases with ω from the resistive to the capacitive percolation regimes.

In view of remark 1, the present example is actually concerned with the network impedance, which has a decreasing magnitude as the frequency increases. To this end, the output equation (20) can be rewritten as

$$u_S(t) = -(H/L)z(t) + (1/L)i(t). \tag{21}$$

By replacing (21) for $u_S(t)$ in (19), it follows that

$$\mathrm{d}z(t)/\mathrm{d}t = (F - NH/L)z(t) + (N/L)i(t). \tag{22}$$

Since the voltage $v(t)$ across the network in figure 7 is given by $v(t) = u_S(t) - R_S i(t)$ and $R_S = 1/L$, it follows from (21) that

$$v(t) = -(H/L)z(t). \tag{23}$$

Therefore, in light of (22) and (23), the complex network impedance is calculated as

$$Z(j\omega) = -(H/L)(j\omega I - F + NH/L)^{-1}N/L. \tag{24}$$

The data for the present study were generated by using the state-space model (22), (23) with the following current waveform:

$$i(t) = 0.2\sin(0.04\pi t) + \sin(0.4\pi t) + 5\sin(4\pi t), \tag{25}$$

which comprises three sinusoids with angular frequencies ranging from approximately 0.1 to 10 rad s^{-1}. The states of the

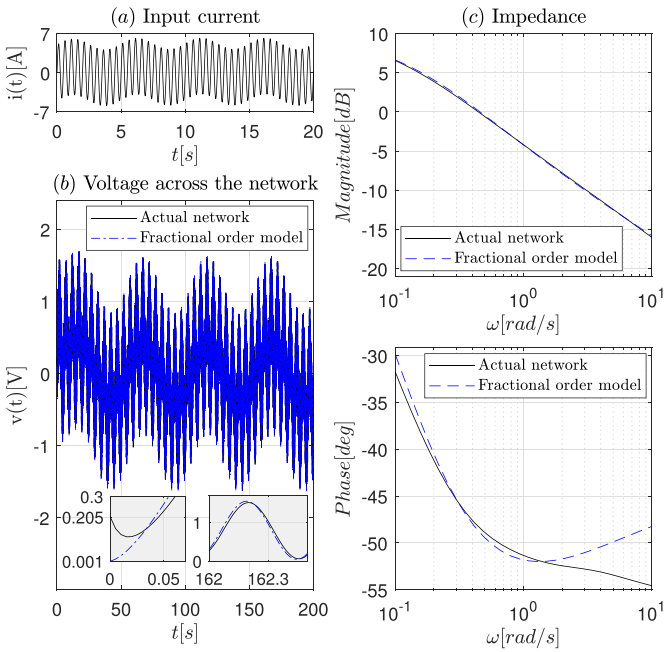

Figure 8. Three-dimensional RC network example. (a) Input signal employed in the identification procedure. (b) Output of the actual network (black solid line) and the identified model (blue dash-dotted line). The insets show enlarged details of the signals at the initial and final parts of the simulation. (c) Magnitude and phase of the actual network impedance (black solid line) and the identified model (blue dashed line).

model were randomly initialized by using a normal distribution with zero mean and unit standard deviation. In what follows, a typical result is presented. The current input $u(t) = i(t)$ and voltage output $y(t) = v(t)$ waveforms thus obtained are presented in figures 8(a) and (b), respectively. In this example, no noise was added to the output signal. The identification was carried out to obtain an impedance transfer function of the form

$$Z(s) = \frac{V(s)}{I(s)} = \frac{b_0 + b_1 s^{\alpha}}{1 + a_1 s^{\alpha} + a_2 s} \tag{26}$$

which has the same structure of the model adopted in [4], after conversion from admittance to impedance form and exclusion of the source resistance.

By using the method proposed in this paper, the identified transfer function was

$$\hat{G}(s) = \frac{2.9539 + 3.5310 s^{0.5303}}{1 + 1.5097 s^{0.5303} + 8.3151 s}, \tag{27}$$

which exhibits good agreement with the actual network impedance, as shown in the frequency-domain plots presented in figure 8(c). As can be seen in the insets in figure 8(b), the model also provides a good match of the network output in the time domain.

On the other hand, the method presented in [5], which does not take into account the non-null initial conditions of the network, resulted in a very different model:

$$\hat{G}(s) = \frac{3.1719 - 0.1137s^{0.9684}}{1 + 44.1407s^{0.9684} - 40.1192s}, \tag{28}$$

which was found to be unstable, in clear contrast with the physical nature of the actual system. This result clearly justifies the benefits of the current refinement from our previous formulations; these are absolutely necessary for the unambiguous identification of this type of system.

5. Conclusion

This contribution extended the exponential modulation technique presented in [5] to the identification of fractional order systems with non-zero initial conditions. To this end, the problem was recast in terms of an artificial system with null initial conditions. Compared to the method presented in [6], the proposed approach has the advantages of handling models with derivatives at the input and allowing for the identification of the fractional exponents. In an example involving a Monte Carlo simulation with measurement noise, the estimated parameters and initial conditions were found to be unbiased and displayed small dispersion around the actual values. In contrast, by using the original method presented in [5], the errors in the parameter estimates were much larger. The proposed method also provided suitable results in an example concerning the identification of the input impedance of a three-dimensional RC network. In this case, the previously reported method was severely affected by the presence of non-zero initial conditions and resulted in an unstable model, whereas this is not the case in the current formulation. The precise identification of RC network dynamics taking into consideration explicitly the initial conditions paves the way for new modelling methodologies that should provide better understanding of the dynamics associated with complex phenomena, as encountered across a range of disciplines such as physics [18], chemistry [19] and biomedical engineering [20–24].

Data availability statement

All data that support the findings of this study are included within the article (and any supplementary files).

Acknowledgments

This work was supported by Conselho Nacional de Desenvolvimento Científico e Tecnológico (CNPq) - Grants 308581/2022-9, 305233/2022-0, 303637/2021-8 and Coordenação de Aperfeiçoamento de Pessoal de Nível Superior (CAPES) – Finance Code 001, Brazil.

Conflict of interest

The authors declare that they have no known competing financial interests or personal relationships that could have appeared to influence the work reported in this technical design note.

CRediT authorship contribution statement

H Kuzminskas: Conceptualization, Software, Writing, Editing, Data curation. M M C Teixeira: Conceptualization, Supervision, Validation, Review. R K H Galvão: Conceptualization, Methodology, Validation, Review. E Assunção: Conceptualization, Validation, Review. S Hadjiloucas: Validation, Review. All authors have read and agreed to this version of the manuscript.

ORCID iDs

Hadamez Kuzminskas https://orcid.org/0000-0002-9792-6752
Marcelo Carvalho Minhoto Teixeira https://orcid.org/0000-0002-2996-2831
Roberto Kawakami Harrop Galvão https://orcid.org/0000-0001-9794-8815
Edvaldo Assunção https://orcid.org/0000-0002-4439-8570
Sillas Hadjiloucas https://orcid.org/0000-0003-2380-6114

References

[1] Sun H, Zhang Y, Baleanu D, Chen W and Chen Y 2018 A new collection of real world applications of fractional calculus in science and engineering *Commun. Nonlinear Sci. Numer. Simul.* **64** 213–31
[2] Wu C, Yang J, Huang D, Liu H and Hu E 2019 Weak signal enhancement by fractional-order system resonance and its application in bearing fault diagnosis *Meas. Sci. Technol.* **30** 035004
[3] Deng Q, Qiu D, Xie Z, Zhang B and Chen Y 2023 Online SOC estimation of supercapacitor energy storage system based on fractional-order model *IEEE Trans. Instrum. Meas.* **72** 1502010
[4] Jacyntho L A, Teixeira M C M, Assunção E, Cardim R, Galvão R K H and Hadjiloucas S 2015 Identification of fractional-order transfer functions using a step excitation *IEEE Trans. Circuits Syst.* II **62** 896–900
[5] Galvão R K H, Teixeira M C M, Assunção E, Paiva H M and Hadjiloucas S 2020 Identification of fractional-order transfer functions using exponentially modulated signals with arbitrary excitation waveforms *ISA Trans.* **103** 10–18
[6] Lu Y, Tang Y, Zhang X and Wang S 2020 Parameter identification of fractional order systems with nonzero initial conditions based on block pulse functions *Measurement* **158** 107684
[7] Sin M H, Sin C, Ji S, Kim S Y and Kang Y H 2022 Identification of fractional-order systems with both nonzero initial conditions and unknown time delays based on block pulse functions *Mech. Syst. Signal Process.* **169** 108646

[8] Wang J C, Liu D Y, Boutat D and Wang Y 2023 An innovative modulating functions method for pseudo-state estimation of fractional order systems *ISA Trans.* **136** 334–44
[9] Podlubny I 1998 *Fractional Differential Equations: an Introduction to Fractional Derivatives, Fractional Differential Equations, to Methods of Their Solution and Some of Their Applications* (Elsevier)
[10] Hadamard J 1892 Essai sur l'étude des fonctions données par leur développement de Taylor *J. de Mathématiques Pures et Appliquées* **8** 101–86
[11] Kilbas A A 2001 Hadamard-type fractional calculus *J. Korean Math. Soc.* **38** 1191–204
[12] Sontakke B and Shaikh A 2015 Properties of Caputo operator and its applications to linear fractional differential equations *Int. J. Eng. Res. Appl.* **5** 22–27
[13] Li C, Li Z and Wang Z 2020 Mathematical analysis and the local discontinuous Galerkin method for Caputo-Hadamard fractional partial differential equation *J. Sci. Comput.* **85** 1–27
[14] Nelder J A and Mead R 1965 A simplex method for function minimization *Comput. J.* **7** 308–13
[15] Xue D 2019 *FOTF Toolbox for Fractional-Order Control Systems Applications in Control* (De Gruyter) pp 237–66
[16] Dorf R C and Bishop R H 2017 *Modern Control Systems* 13th edn (Pearson Education)
[17] Galvão R K H, Hadjiloucas S, Kienitz K H, Paiva H M and Afonso R J M 2013 Fractional order modeling of large three-dimensional RC networks *IEEE Trans. Circuits Syst.* I **60** 624–37
[18] Tarasov V E 2013 Review of some promising fractional physical models *Int. J. Mod. Phys.* B **27** 1330005
[19] Gude J J, Bringas P G, Herrera M, Rincón L, Di Teodoro A and Camacho O 2024 Fractional-order model identification based on the process reaction curve: a unified framework for chemical processes *Results Eng.* **21** 101757
[20] Magin R 2004 Fractional calculus in bioengineering, part 1 *Crit. Rev. Biomed. Eng.* **32** 104
[21] Magin R 2004 Fractional calculus in bioengineering, part 2 *Crit. Rev. Biomed. Eng.* **32** 90
[22] Magin R 2004 Fractional calculus in bioengineering, part 3 *Crit. Rev. Biomed. Eng.* **32** 183
[23] Freeborn T J 2013 A survey of fractional-order circuit models for biology and biomedicine *IEEE J. Emerg. Sel. Top. Circuits Syst.* **3** 416–24
[24] Matlob M A and Jamali Y 2019 The concepts and applications of fractional order differential calculus in modeling of viscoelastic systems: a primer *Crit. Rev. Biomed. Eng.* **47** 249–76